Electronic Supplementary Material (ESI) for RSC Advances.

Near-infrared luminescence of Nd^{3+} and Yb^{3+} complexes using a polyfluorinated pyrene-based β-diketonate ligand

T. M. George,[a,b] S. Varughese,[b] and M. L. P. Reddy[a,b]*

[a]AcSIR-Academy of Scientific & Innovative Research, CSIR-NIIST Campus, Thiruvananthapuram, India

[b]Materials Science and Technology Division, National Institute for Interdisciplinary Science and Technology (NIIST), Council of Scientific and Industrial Research (CSIR), Thiruvananthapuram-695 019, India, E-mail: mlpreddy55@gmail.com

Contents

Synthetic procedure

Figures

Fig. S17 ESI-MS spectrum of the complex La(hfpyr)$_3$(H_2O).

Fig. S18 ESI-MS spectrum of the complex La(hfpyr)$_3$(bath).

Fig. S19 FT-IR spectra for the complex La(hfpyr)$_3$(H_2O).

Fig. S20 FT-IR spectra for the complex La(hfpyr)$_3$(bath).

Fig. S21 Thermogravimetric curves for complexes Nd(hfpyr)$_3$(H_2O) **1** and Yb(hfpyr)$_3$(H_2O) **3**.

Fig. S22 Thermogravimetric curves for complexes Gd(hfpyr)$_3$(H_2O) **5**.

Fig. S23 Thermogravimetric curves for complexes Nd(hfpyr)$_3$(bath) **2**.

Fig. S24 Thermogravimetric curves for complexes Yb(hfpyr)$_3$(bath) **4**.

Fig. S25 Life time decay profile for complex Gd(hfpyr)$_3$(H_2O) **5** monitored at approximately 514 nm (λ_{ex} = 375 nm) at 298 K**.**

Fig. S26 Life time decay profile for complex Gd(hfpyr)$_3$(H_2O) **5** monitored at approximately 637 nm (λ_{ex} = 375 nm) at 77 K**.**

Fig. S27 Emission spectra for the ligand Hhfpyr, Nd(hfpyr)$_3$(H_2O) **1** and Nd(hfpyr)$_3$(bath) **2** in the visible range (λ_{ex} = 400 nm) at 298 K**.**

Fig. S28 Emission spectra for the ligand Hhfpyr, Yb(hfpyr)$_3$(H_2O) **3** and Yb(hfpyr)$_3$(bath) **4** in the visible range (λ_{ex} = 400 nm) at 298 K**.**

Fig. S29 FT-IR Spectra of the complex Yb(hfpyr)$_3$(bath), PMMA and PMMA film doped with complex **4.**

Fig. S30 Thermogravimetric curve for the PMMA film doped with Yb(hfpyr)$_3$(bath) **4.**

Fig. S31 Life time decay profiles for Yb(hfpyr)$_3$(bath) **4**, doped into PMMA polymer where emission monitored around 979 nm. The straight lines are the best fits considering single-exponential behavior.

Synthetic procedure for the preparation of the complex La(hfpyr)$_3$(H_2O).

To a methanolic solution of Hhfpyr (12 mmol), 12 mmol of NaOH in water was added and stirred for 5 min. La(NO_3)$_3$·6(H_2O) in 3 mL of water (4 mmol) was added drop-wise to the above reaction mixture and stirred for 24 h at 298K. The resultant crude precipitate was filtered, washed with water and dried. The obtained metal complex was recrystallized from chloroform solution.

La(hfpyr)$_3$(H_2O). Elemental analysis (%): calculated for $C_{66}H_{32}F_{21}O_8La$ (1474.83): C 53.75, H 2.19; Found: C 53.68, H 2.28. ^{1}H NMR ($CDC1_3$, 500 MHz) δ (ppm): 8.49 (s, 3H), 8.02 (d, 18H), 7.40 (s, 3H), 7.02 (s, 3H), 6.51 (s, 3H). FT-IR (KBr) ν_{max} (cm^{-1}): 3424, 1611, 1512, 1345, 1229, 1153, 1066, 1033, 966, 847, 750, 667, 536. *m/z* = 1457.09 [La(hfpyr)$_3$+1]$^+$.

Synthetic procedure for the preparation of the complex La(hfpyr)$_3$(bath)

The ternary La^{3+} complex was synthesized by mixing equimolar solutions of the corresponding binary complex and an ancillary ligand, bathophenanthroline (bath) in $CHCl_3$ solution and the resultant mixture was stirred for 12 h at 70°C. The metal complex was then isolated after the removal of solvent by evaporation process. Finally, the ternary lanthanide complex was obtained by recrystallization from chloroform solution.

La(hfpyr)$_3$(bath). Elemental analysis (%): calculated for $C_{90}H_{46}F_{21}N_2O_8La$ (1788.21): C 60.42, H 2.59, N 1.57; Found: C 60.53, H 2.66 N 1.48. ^{1}H NMR ($CDC1_3$, 500 MHz) δ (ppm): 9.57 (s, 2H), 8.72 (m, 3H), 8.13 (m, 4H), 8.08 (m, 3H), 7.99 (m, 5H), 7.84 (m, 6H) 7.48-7.37 (m, 17H), 6.99 (m, 3H) 6.49 (s, 3H). FT-IR (KBr) ν_{max} (cm^{-1}): 3037, 1608, 1541, 1511, 1464, 1343, 1262, 1227, 1029, 969, 849, 762, 668, 595. *m/z* = 1788.53 [La(hfpyr)$_3$(bath)]$^+$.

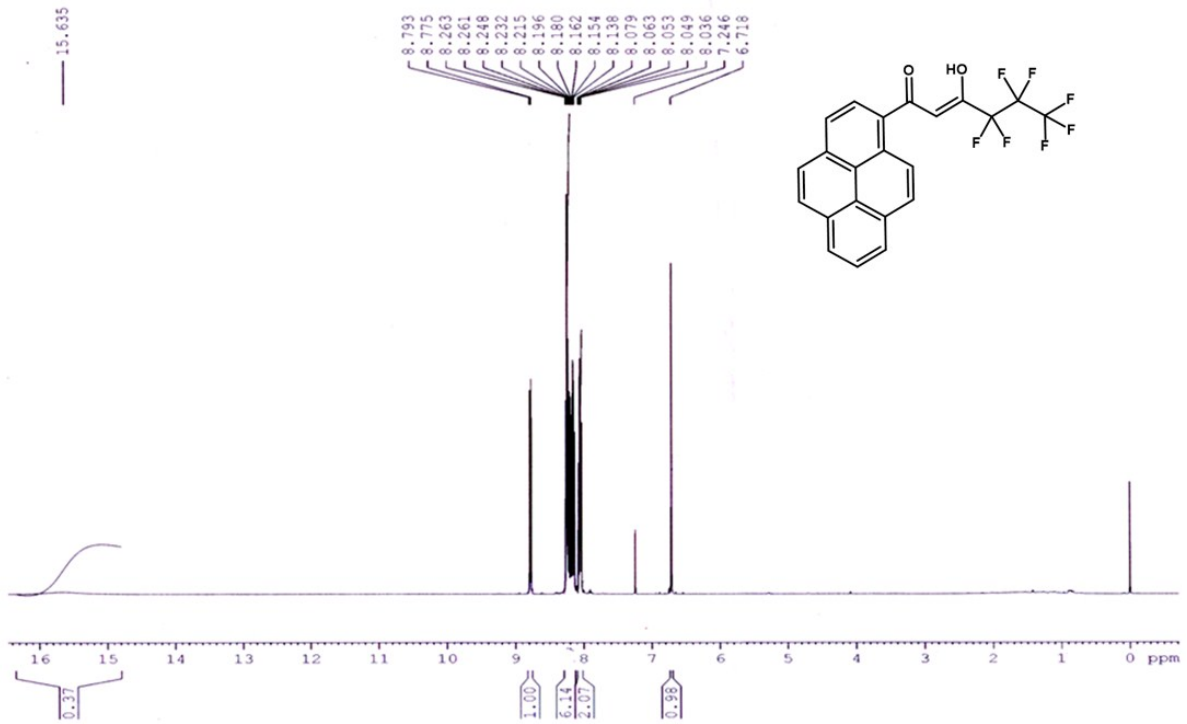

Fig. S1 ^{1}H NMR spectrum of the ligand Hhfpyr**.**

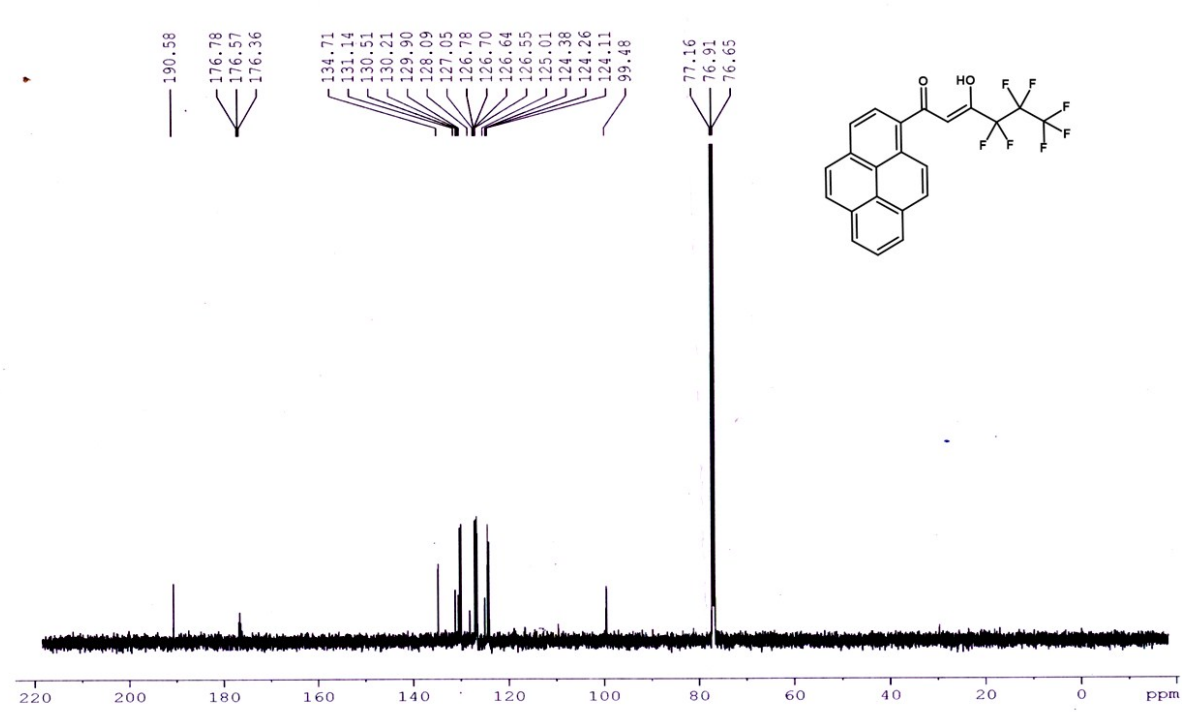

Fig. S2 ^{13}C NMR spectrum of the ligand Hhfpyr.

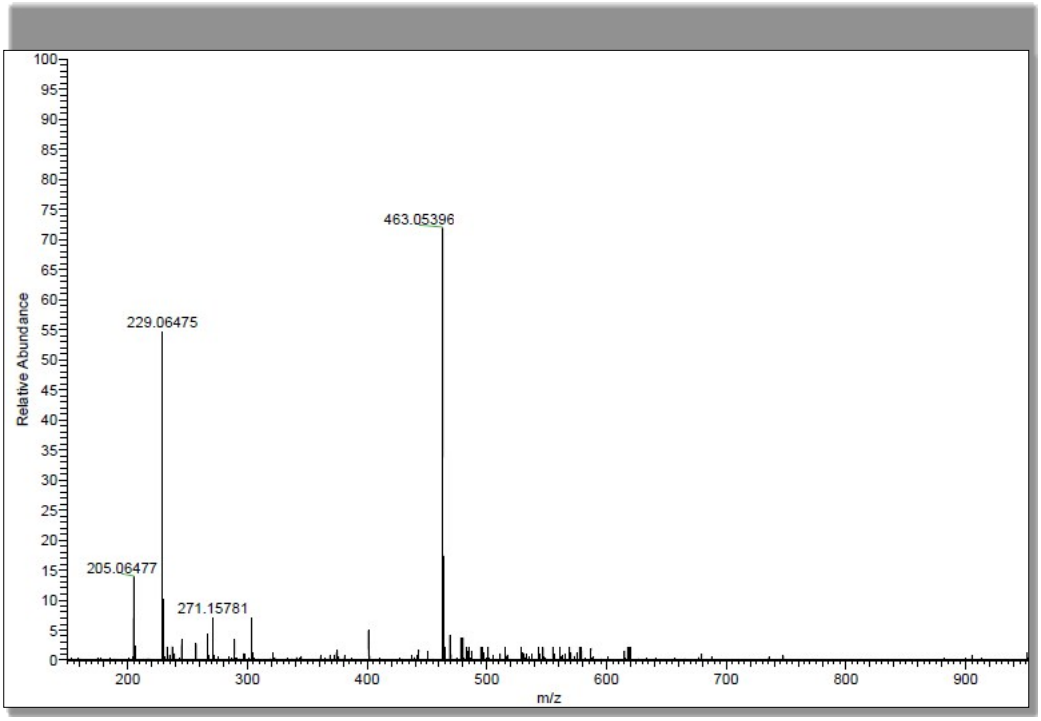

Fig. S3 ESI-MS spectrum of the ligand Hhfpyr.

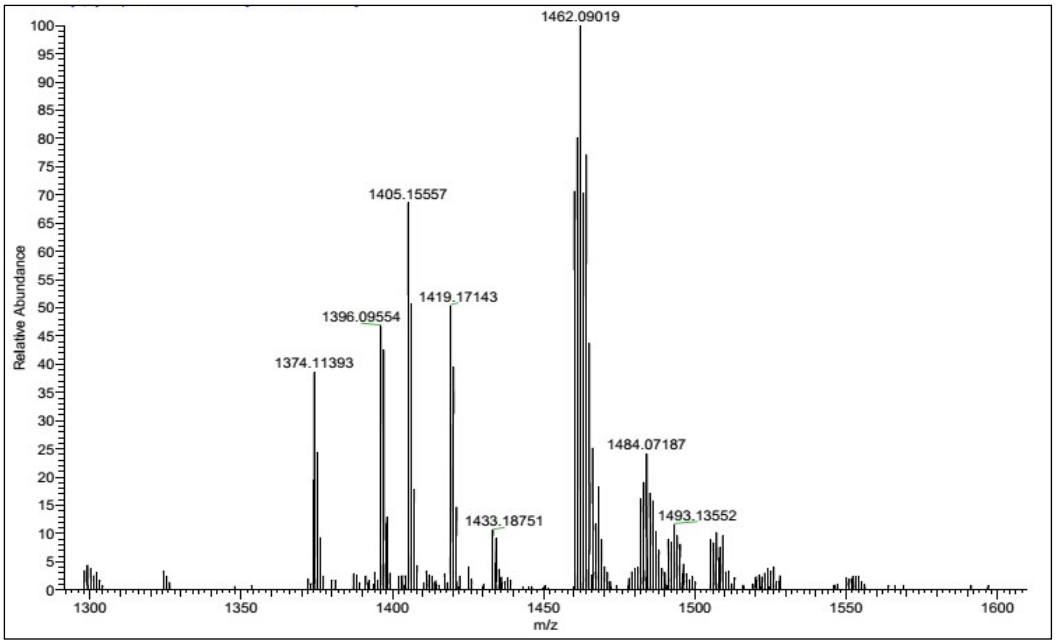

Fig. S4 ESI-MS spectrum of Nd(hfpyr)$_3$(H_2O) **1.**

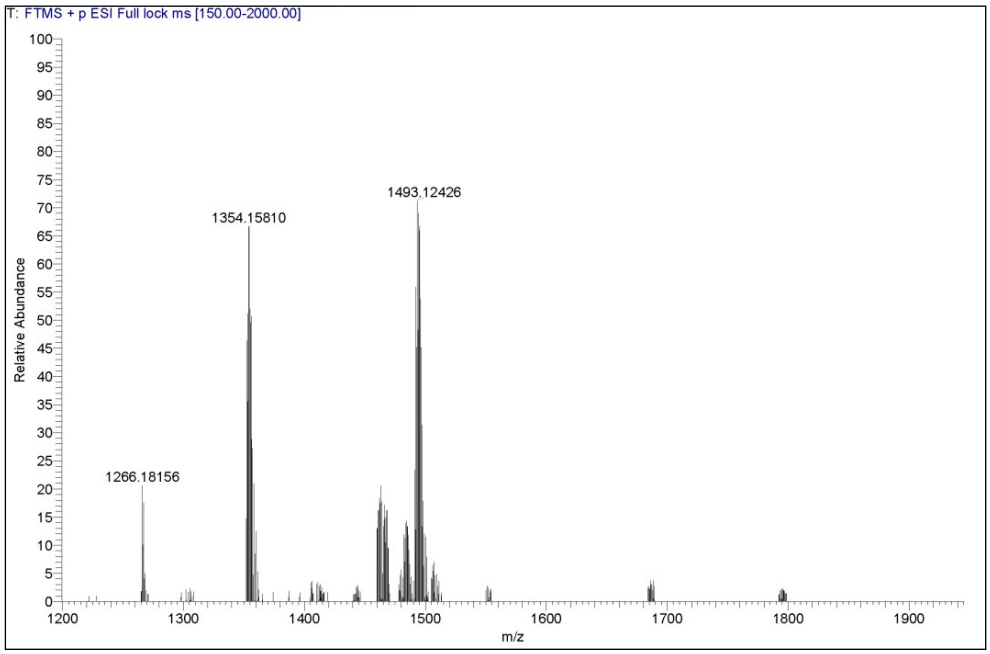

Fig. S5 ESI-MS spectrum of the complex Yb(hfpyr)$_3$(H_2O) **3**.

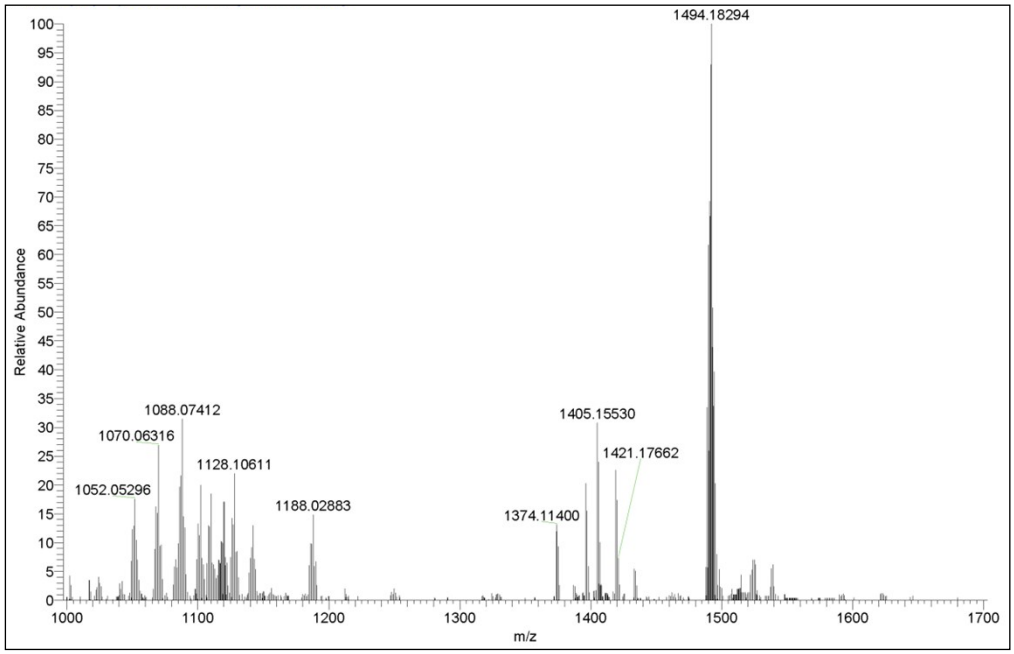

Fig. S6 ESI-MS spectrum of the complex Gd(hfpyr)$_3$(H_2O) **5.**

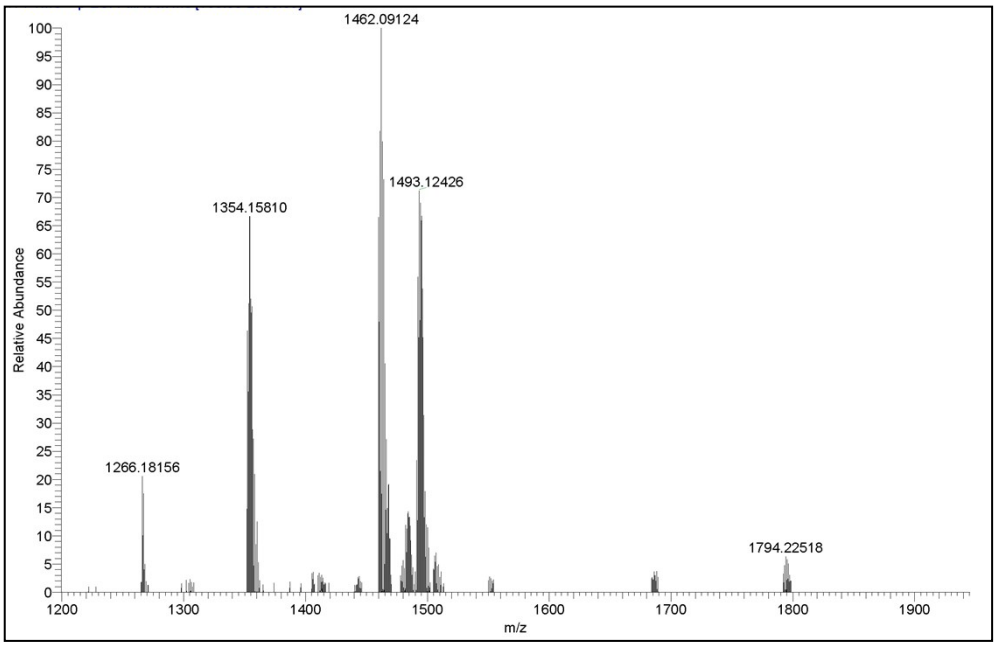

Fig. S7 ESI-MS spectrum of the complex Nd(hfpyr)$_3$(bath) **2**.

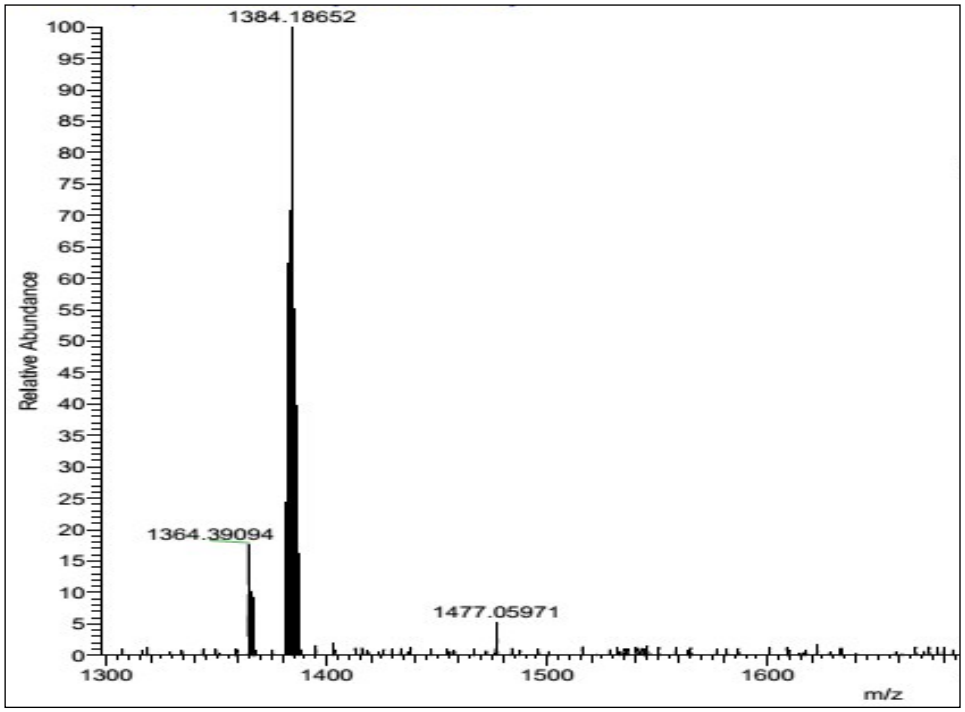

Fig. S8 ESI-MS spectrum of the complex Nd(hfpyr)$_3$(bath) **4**.

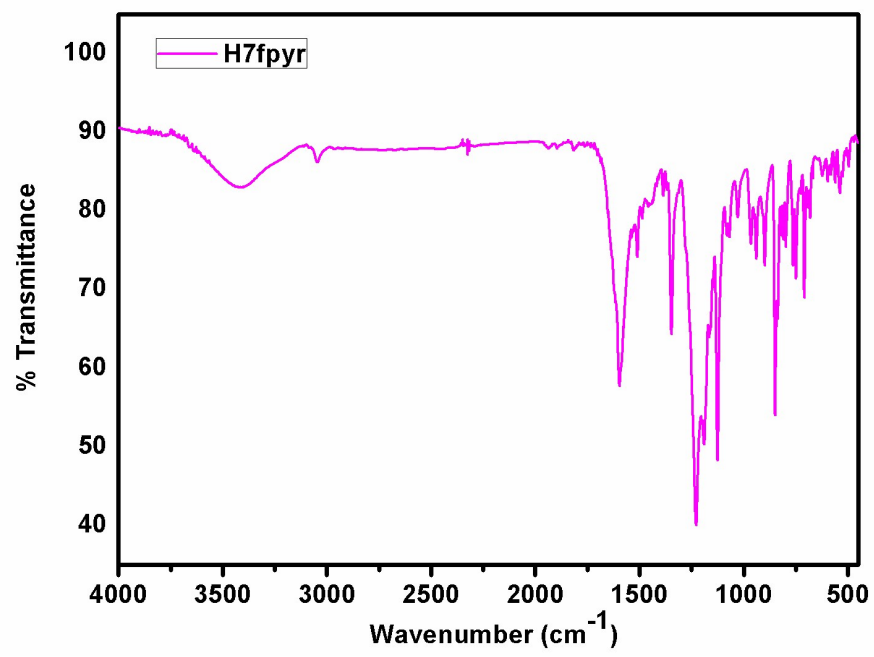

Fig. S9 FT-IR Spectra for the ligand Hhfpyr.

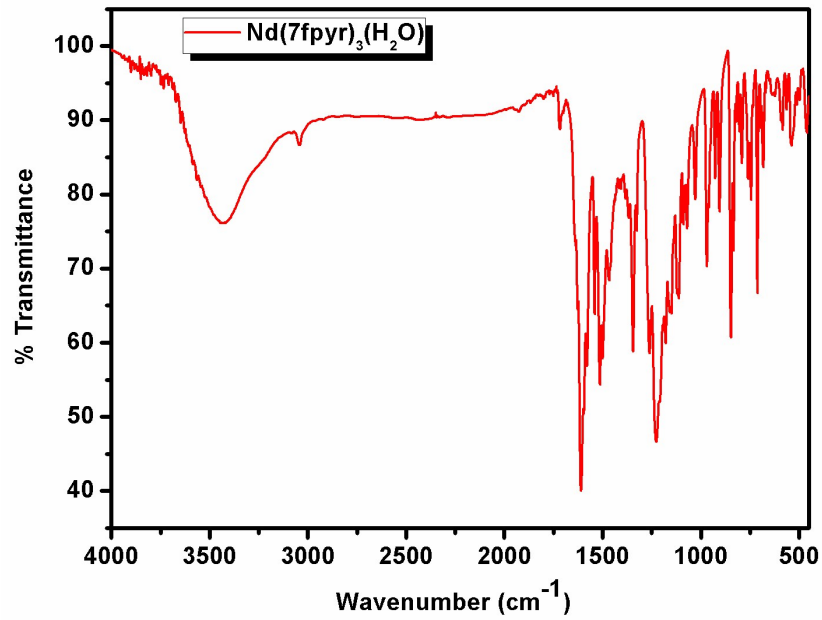

Fig. S10 FT-IR Spectra for the complex Nd(hfpyr)$_3$(H_2O) **1**.

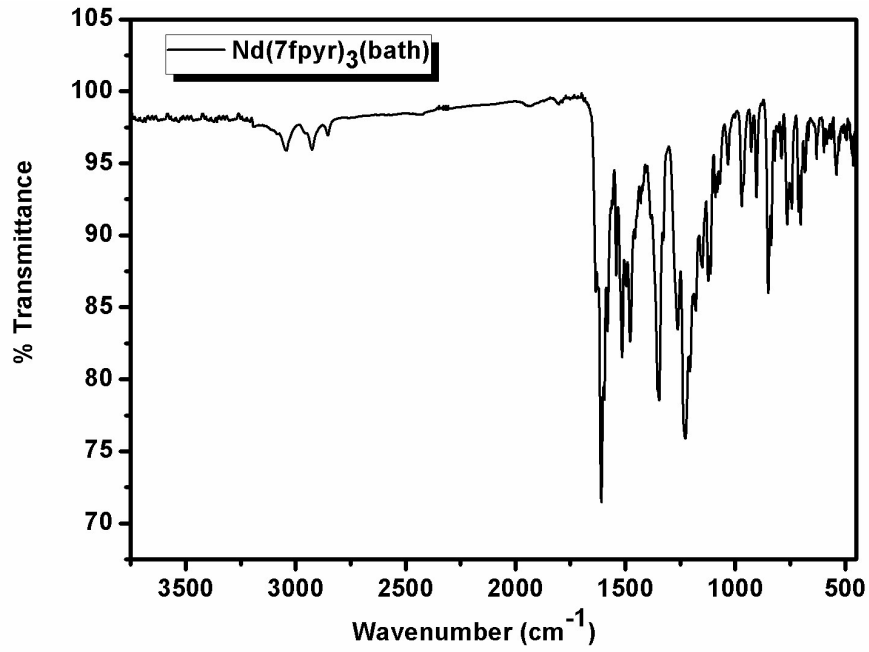

Fig. S11 FT-IR Spectra for the complex Nd(hfpyr)$_3$(bath) **2**.

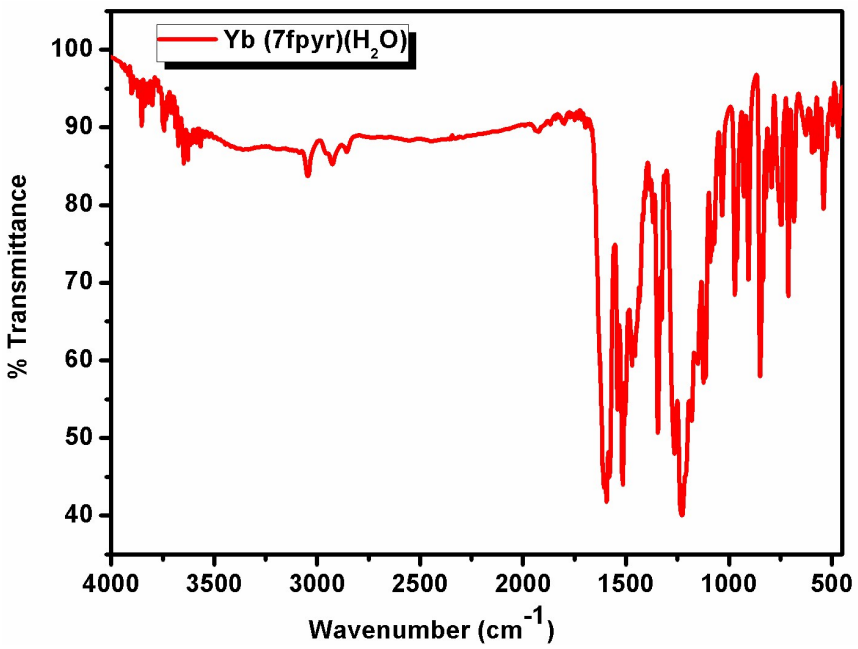

Fig. S12 FT-IR Spectra for the complex Yb(hfpyr)$_3$(H_2O) **3**.

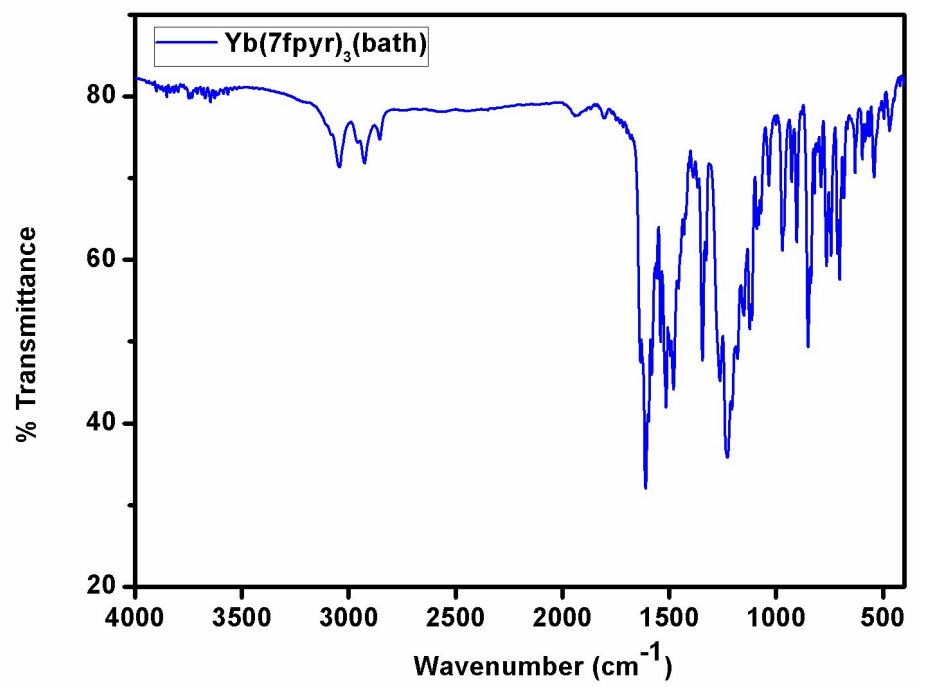

Fig. S13 FT-IR Spectra for the complex Yb(hfpyr)$_3$(bath) **4**.

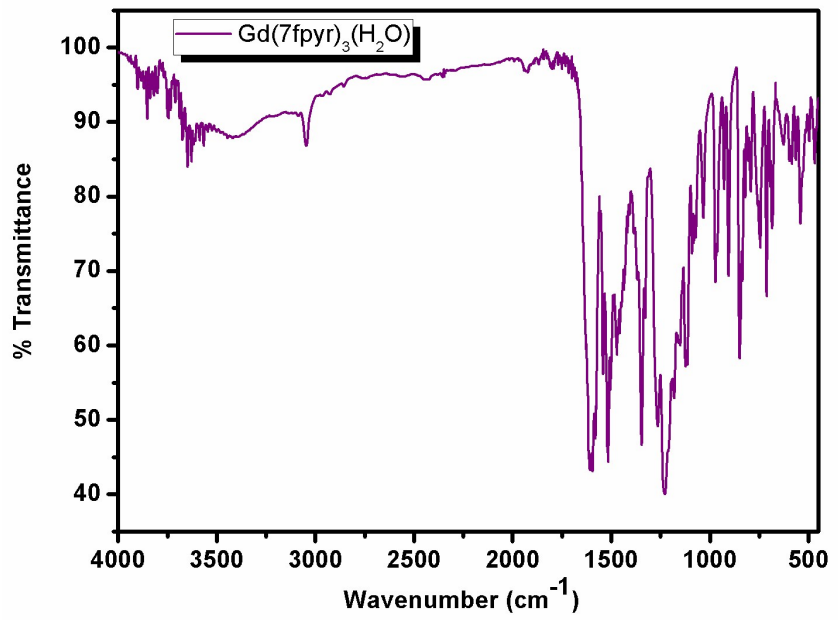

Fig. S14 FT-IR Spectra for the complex Gd(hfpyr)$_3$(H_2O) **5**.

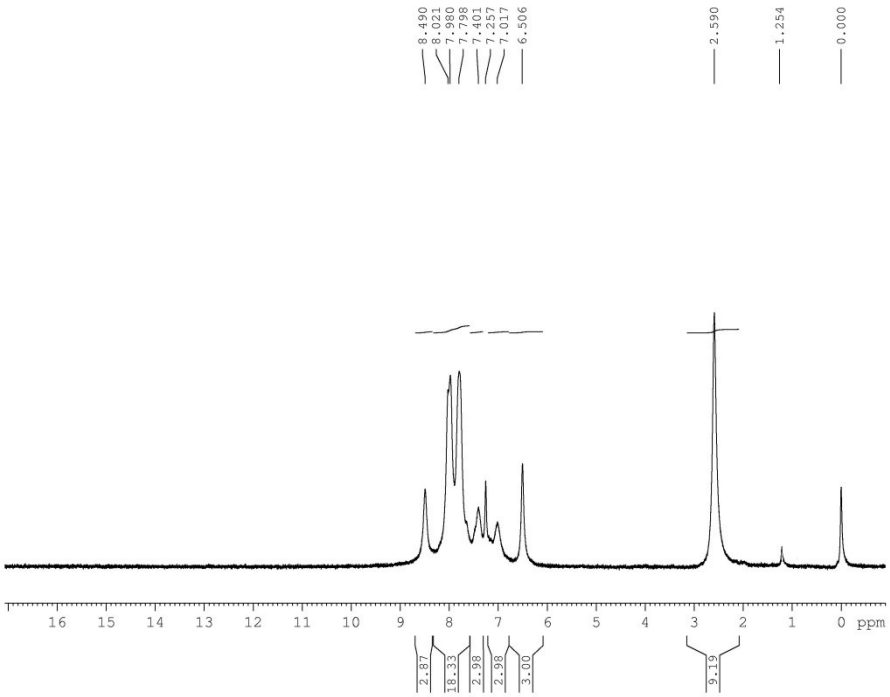

Fig. S15 ^{1}H NMR spectrum of the complex La(hfpyr)$_3$(H_2O).

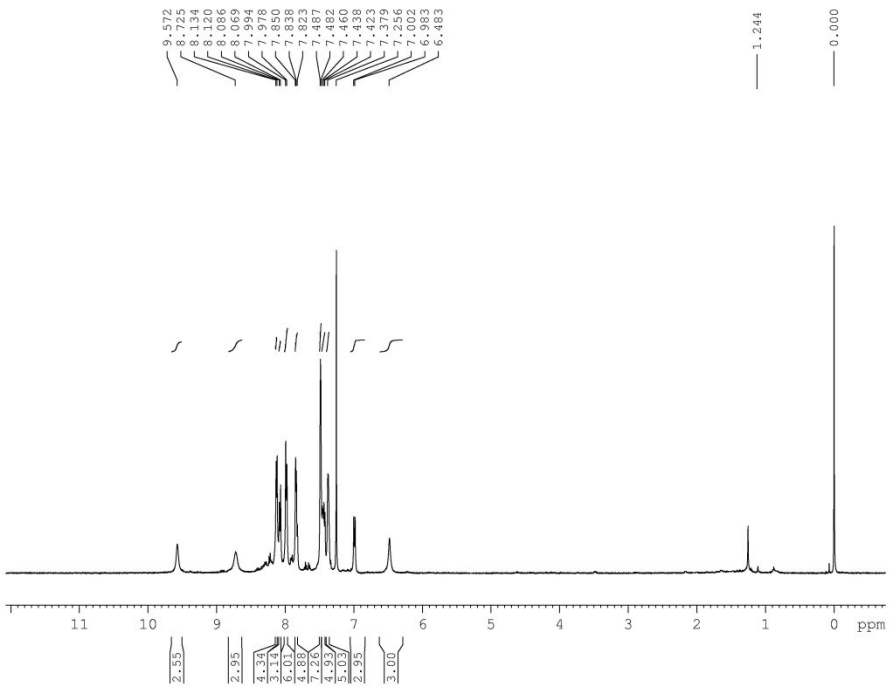

Fig. S16 ^{1}H NMR spectrum of the complex La(hfpyr)$_3$(bath).

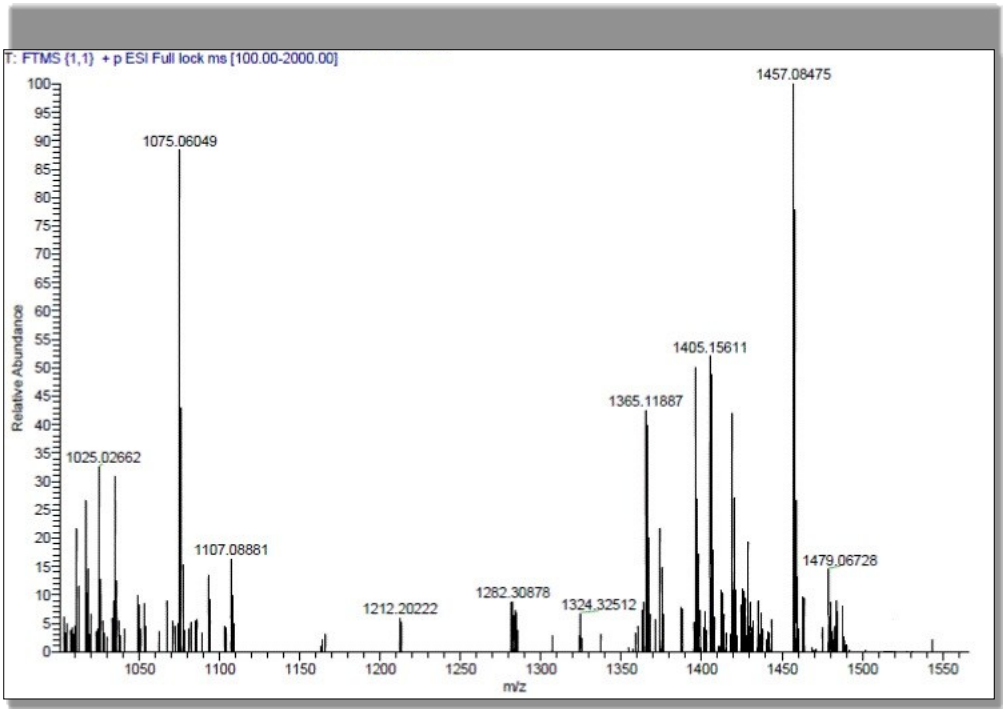

Fig. S17 ESI-MS spectrum of the complex La(hfpyr)$_3$(H_2O).

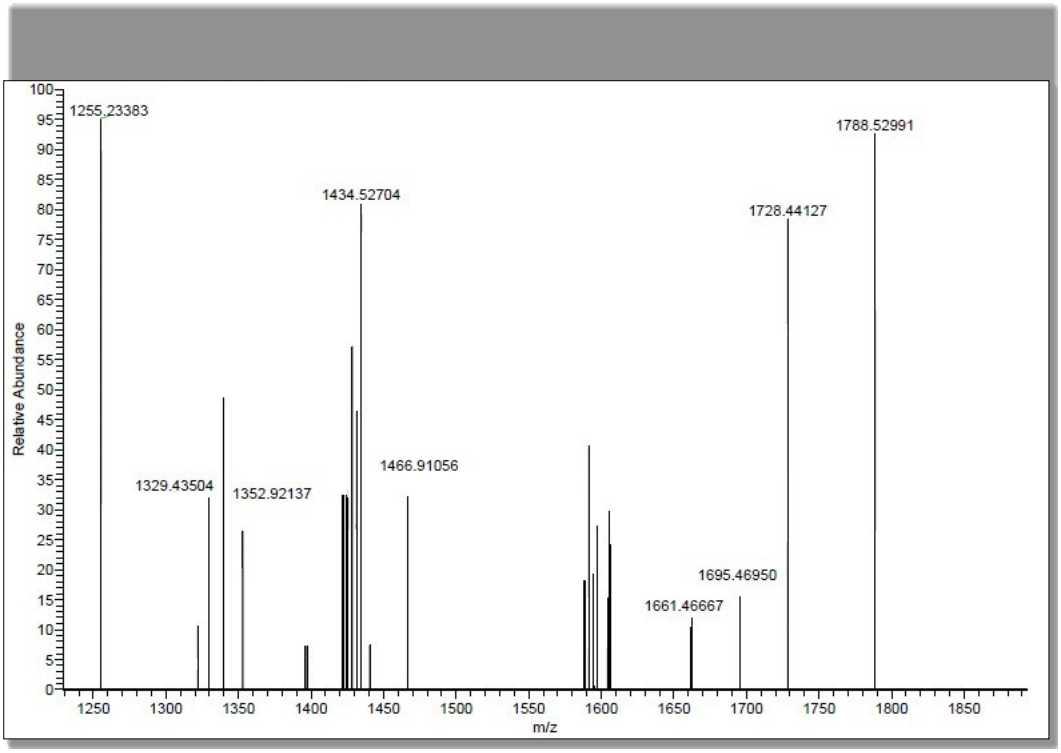

Fig. S18 ESI-MS spectrum of the complex La(hfpyr)$_3$(bath).

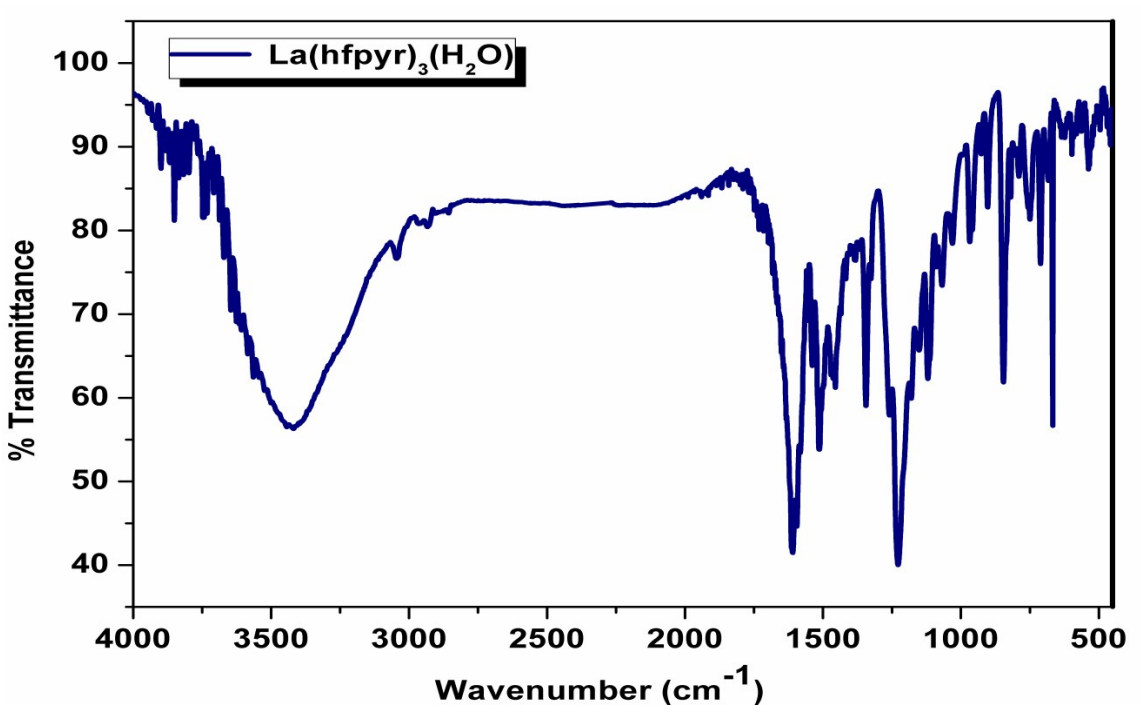

Fig. S19 FT-IR spectra for the complex La(hfpyr)$_3$(H_2O).

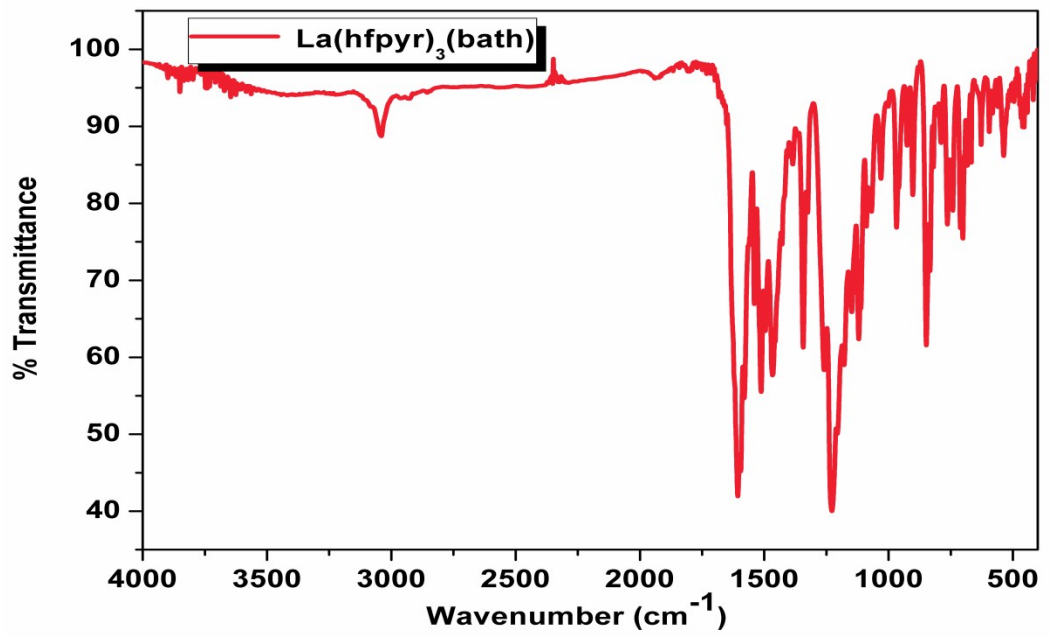

Fig. S20 FT-IR spectra for the complex La(hfpyr)$_3$(bath).

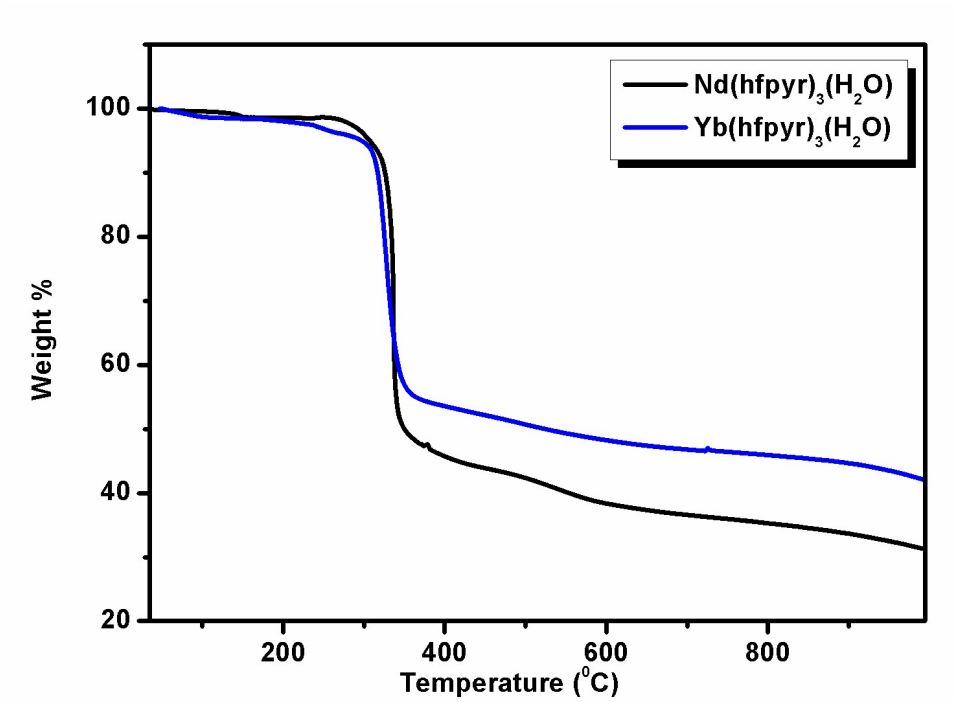

Fig. S21 Thermogravimetric curves for complexes Nd(hfpyr)$_3$(H$_2$O) **1** and Yb(hfpyr)$_3$(H$_2$O) **3**.

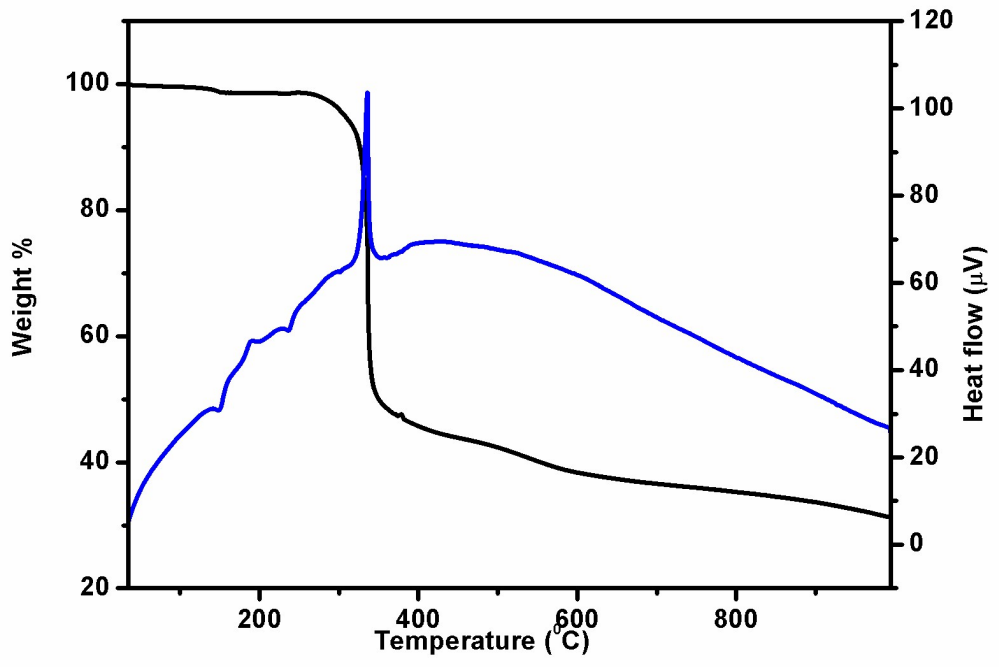

Fig. S22 Thermogravimetric curves for complexes Gd(hfpyr)$_3$(H$_2$O) **5**.

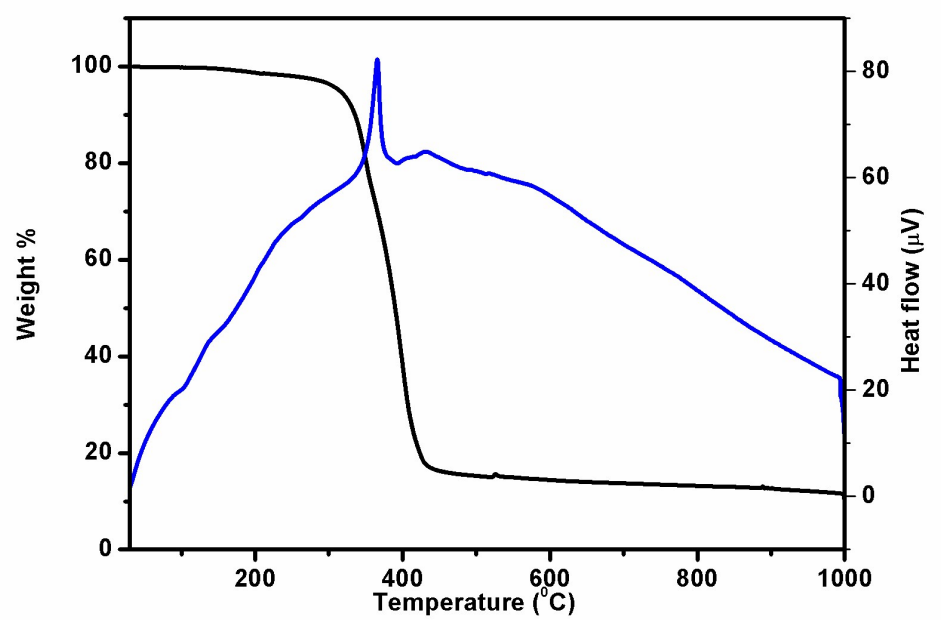

Fig. S23 Thermogravimetric curves for complexes $Nd(hfpyr)_3(bath)$ **2.**

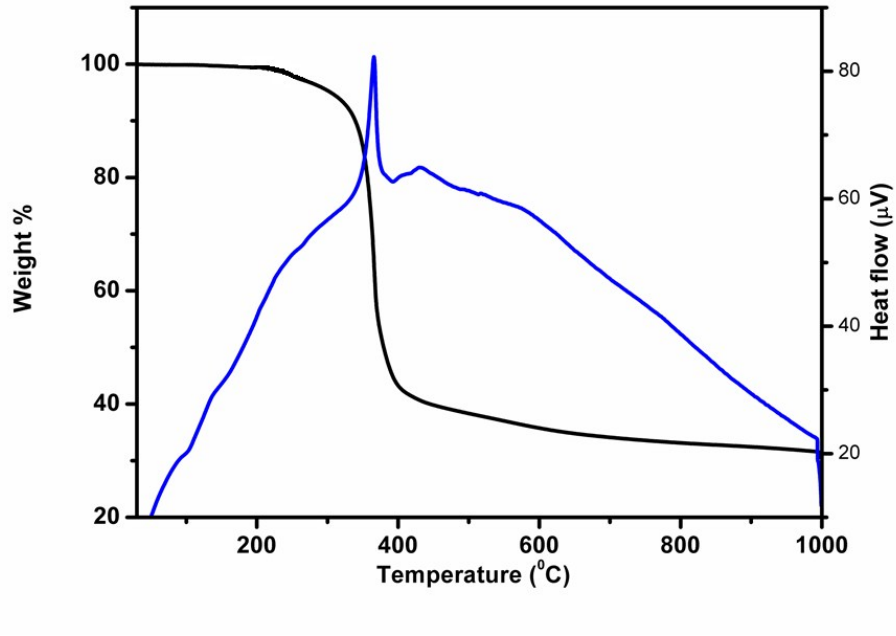

Fig. S24 Thermogravimetric curves for complexes $Yb(hfpyr)_3(bath)$ **4.**

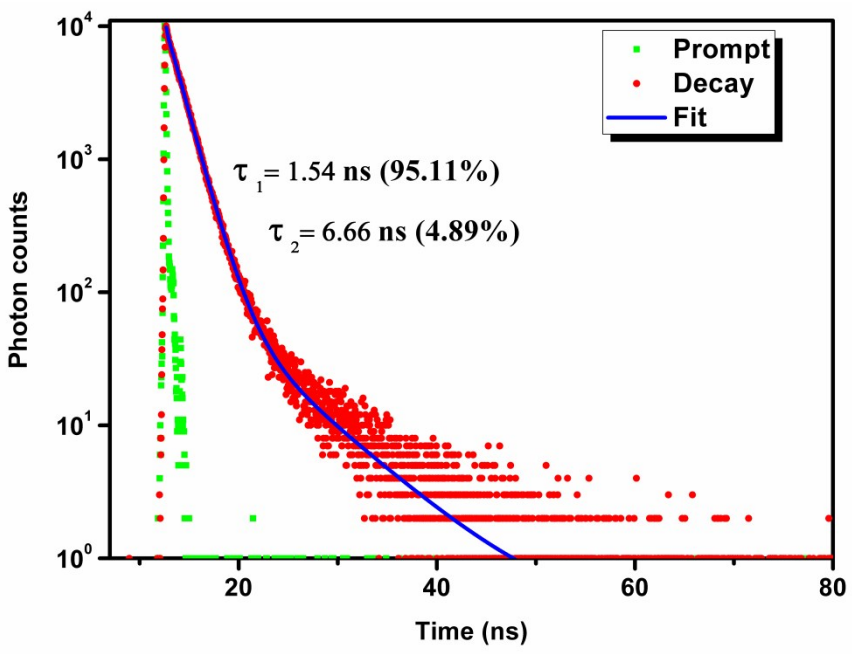

Fig. S25 Life time decay profile for complex Gd(hfpyr)$_3$(H_2O) **5** in THF solution (*c* = 1 x 10^{-5} M) monitored at approximately 514 nm (λ_{ex} = 375 nm) at 298 K**.**

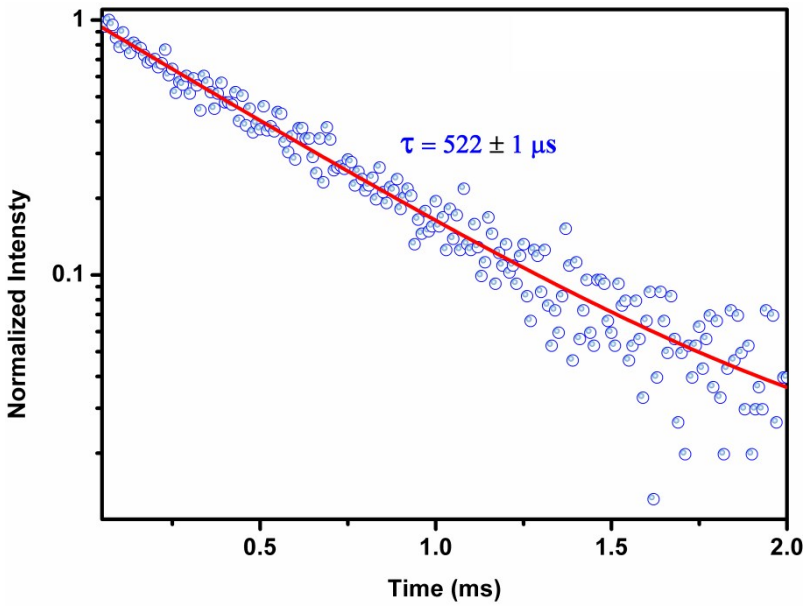

Fig. S26 Life time decay profile for complex Gd(hfpyr)$_3$(H_2O) **5** monitored at approximately 637 nm (λ_{ex} = 375 nm) at 77 K**.**

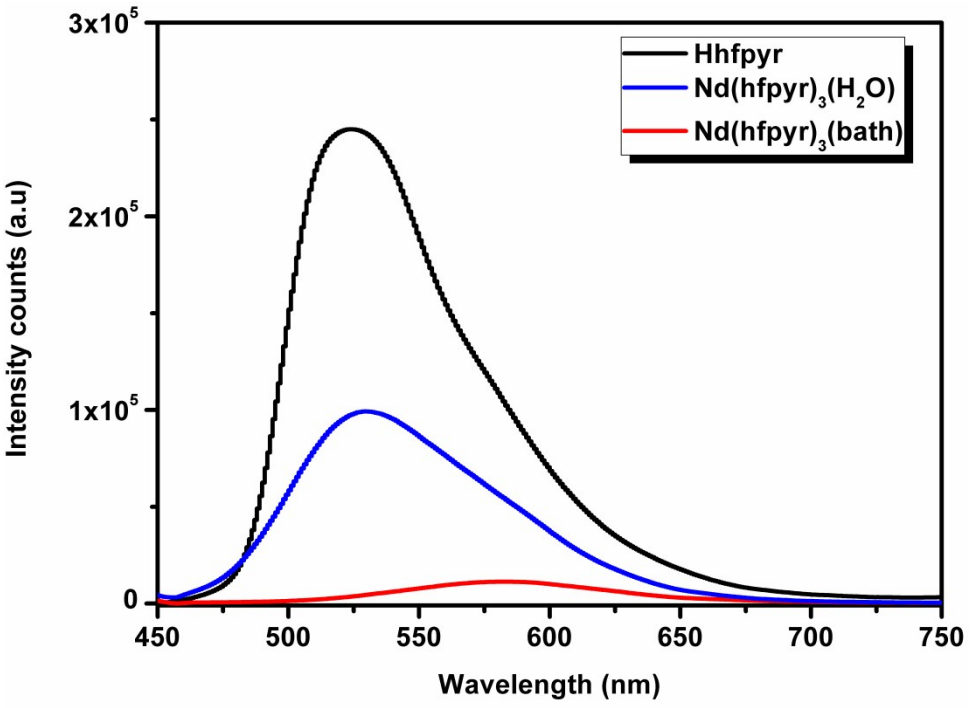

Fig. S27 Emission spectra for the free ligand Hhfpyr, Nd(hfpyr)$_3$(H$_2$O) **1** and Nd(hfpyr)$_3$(bath) **2** in the visible range (λ_{ex} = 400 nm) at 298 K**.**

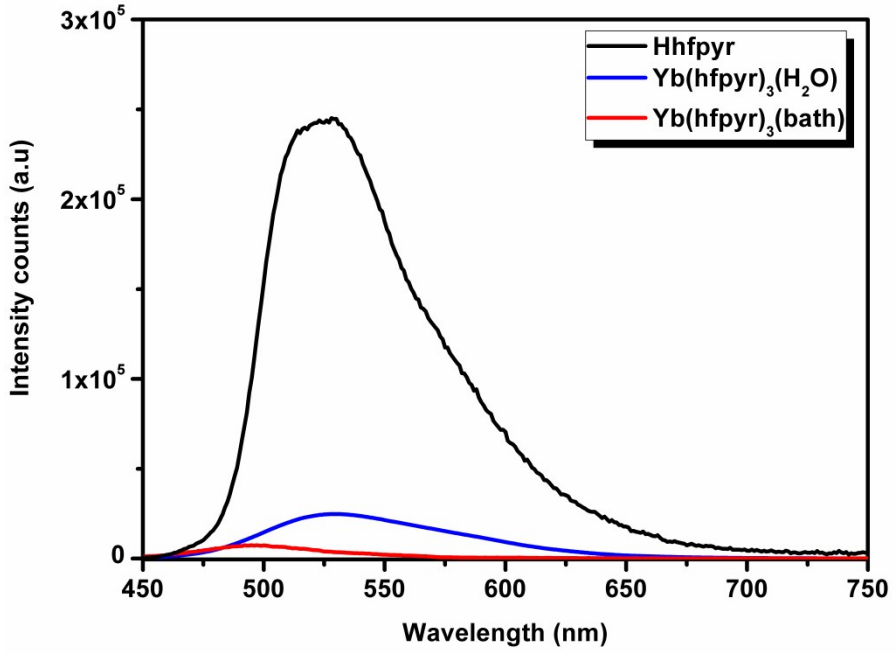

Fig. S28 Emission spectra for the free ligand Hhfpyr, Yb(hfpyr)$_3$(H$_2$O) **3** and Yb(hfpyr)$_3$(bath) **4** in the visible range (λ_{ex} = 400 nm) at 298 K**.**

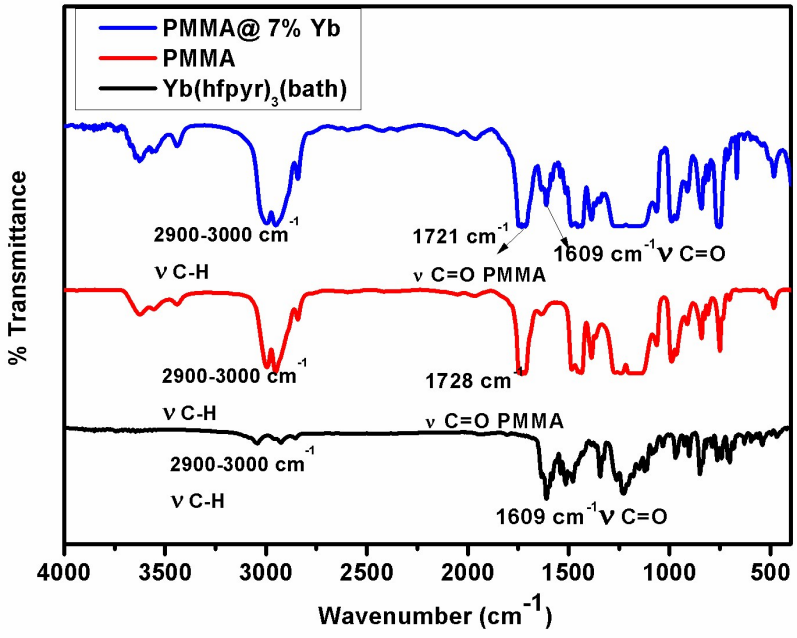

Fig. S29 FT-IR Spectra of the complex Yb(hfpyr)$_3$(bath), PMMA and PMMA film doped with complex **4.**

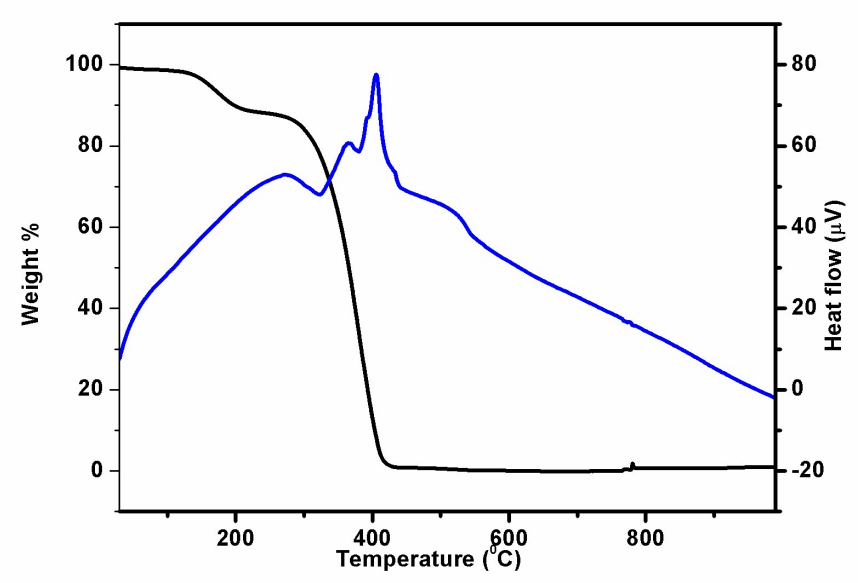

Fig. S30 Thermogravimetric curve for the PMMA film doped with Yb(hfpyr)$_3$(bath) **4.**

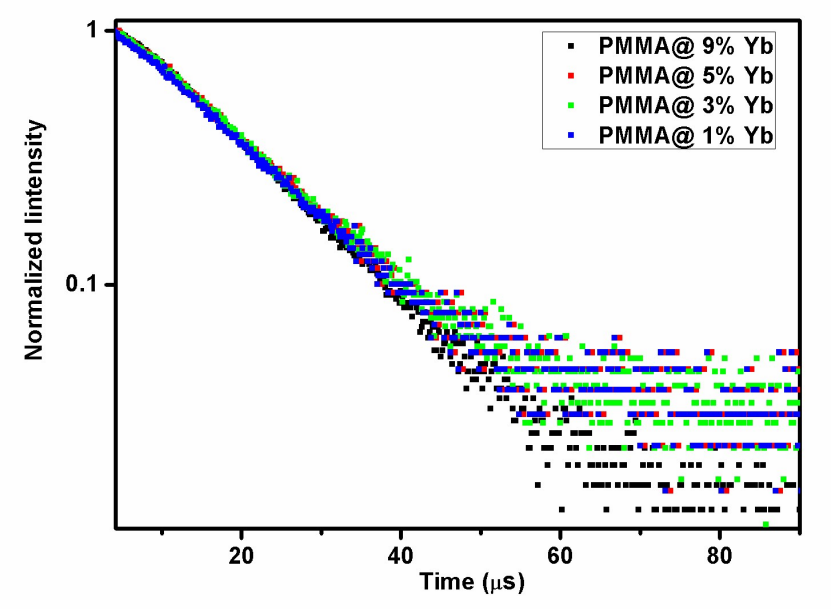

Fig. S31 Life time decay profiles for Yb(hfpyr)$_3$(bath) **4**, doped into PMMA polymer where emission monitored around 979 nm. The straight lines are the best fits considering single-exponential behavior.